Letter Editors' Suggestion

Spread complexity rate as proper momentum

Pawel Caputa,[1,2,3] Bowen Chen,[4,2] Ross W. McDonald,[5] Joan Simón,[5] and Benjamin Strittmatter[5]

[1]*The Oscar Klein Centre and Department of Physics, Stockholm University, AlbaNova, 106 91 Stockholm, Sweden*

[2]*Faculty of Physics, University of Warsaw, Pasteura 5, 02-093 Warsaw, Poland*

[3]*Yukawa Institute for Theoretical Physics, Kyoto University, Kitashirakawa Oiwakecho, Sakyo-ku, Kyoto 606-8502, Japan*

[4]*Kavli Institute for Theoretical Sciences, University of Chinese Academy of Sciences, Beijing 100190, China*

[5]*School of Mathematics and Maxwell Institute for Mathematical Sciences, University of Edinburgh, Edinburgh EH9 3FD, United Kingdom*

(Received 19 November 2024; accepted 14 January 2026; published 11 February 2026)

We demonstrate a precise relation between the rate of complexity of quantum states excited by local operators in two-dimensional conformal field theories and the radial momentum of particles in three-dimensional anti–de Sitter spacetimes. Similar relations have been anticipated based on qualitative models for operator growth. Here, we make this correspondence sharp with two key ingredients: the precise definition of quantum complexity given by the spread complexity of states, and the match of its growth rate to the bulk momentum measured in the proper radial distance coordinate.

DOI: 10.1103/7zs8-9zpg

Introduction. Complexity, a cornerstone of information theory and computation [1–5], has become increasingly important for understanding quantum dynamics. In searching for a physical definition of complexity, we aim to find an observable that captures the difficulty of preparing a quantum state. This has been a focus of interdisciplinary research for many years [6–23].

Surprisingly, complexity may also be the key to understanding black hole interiors. As first noticed in [24], the linear growth with time of generic black hole interiors, probed by extremal surfaces, might be a manifestation of their complexity and ability to process information. Such deep statements can only be tested within a quantum theory of gravity and, indeed, the AdS/CFT correspondence [25] has already provided some supporting evidence [26–29].

A concrete outcome of these developments is a conjecture stating that the rate of growth of complexity is proportional to the radial momentum of massive particles in anti–de Sitter (AdS) spacetimes [30–40]

$$\dot{C}(t) \equiv \frac{d}{dt}C(t) \propto P, \qquad (1)$$

where $C(t)$ captures the effective size of Heisenberg operators $\mathcal{O}(t,x)$ [41].

The main challenge in advancing this program has been the lack of a precise definition of quantum complexity [the left side of (1)] in quantum field theory (QFT), and matching it with momentum on the gravity side [the right side of (1)].

Since Heisenberg evolution of quantum operators is ubiquitous in physics, many new approaches to quantum complexity and operator growth have been developed [49–52]. When working on a 1D chain, there is a natural notion of size related to the support of a given operator as time flows. This picture was developed within the Sachdev-Ye-Kitaev (SYK) model [53,54] in [55,56] and relation (1) was demonstrated within a gauge invariant formulation of a quantum point particle in AdS_2 [40]. Still, it was not clear what size in the SYK model has to do with complexity or how to generalize the setup to higher-dimensional, interacting conformal field theories (CFTs) in conventional holography.

Important progress on defining operator complexity was achieved in many-body physics [52] by using the Krylov basis and Krylov complexity (see, e.g., [57–66]). Furthermore, its dependence on the choice of inner product in the space of operators [67] was circumvented by introducing the spread complexity (reviewed below) of the unitary evolution of quantum states [68]. The first tests of this new complexity measure in SYK models [69,70] provided evidence of its relevance in holography and quantum gravity.

In this Letter, we report a new milestone in this program by explicitly demonstrating (1) in an AdS/CFT setup. Namely, we compute the rate of growth of the spread complexity of locally excited states in 2D CFTs and match it with the proper radial momentum of the dual massive particle in AdS_3. This elevates (1) from a low-dimensional observation to a new entry in the quantum information chapter of the holographic dictionary [see formula (28)].

Complexity of spread of states. The concepts of Krylov and spread complexity [68] extend the intuitive notion of operator size on a lattice to arbitrary quantum systems. The key idea (called the recursion method, [71]) is to map the quantum dynamics to motion on an effective one-dimensional chain spanned by the Krylov basis, vs, the subspace of orthonormal states $\{|K_n\rangle\}$ visited during the Hamiltonian evolution of the initial state

$$|\psi(t)\rangle = e^{-iHt}|\psi_0\rangle = \sum_n \psi_n(t)|K_n\rangle. \tag{2}$$

The Krylov basis is obtained by applying the Lanczos algorithm [72] to the Krylov subspace $\{|\psi_0\rangle, H|\psi_0\rangle, H^2|\psi_0\rangle, \ldots\}$. By construction, the coefficients in the Krylov basis, $\psi_n(t)$ satisfy a discrete Schrödinger equation

$$i\partial_t\psi_n(t) = a_n\psi_n(t) + b_n\psi_{n-1}(t) + b_{n+1}\psi_{n+1}(t), \tag{3}$$

controlled by the Lanczos coefficients a_n and b_n. These are a byproduct of the Lanczos algorithm, and can also be extracted from the moments of the return amplitude

$$S(t) = \langle\psi(t)|\psi_0\rangle. \tag{4}$$

The sites of the one-dimensional chain emerging in (3) are labeled by the Krylov index n, and the Lanczos coefficients describe the probability amplitude of staying on a given site (a_n) or hopping to the neighboring sites (b_n). Solving (3) yields the probability distribution $p_n(t) = |\psi_n(t)|^2$, capturing the entire quantum dynamics.

The spread complexity is defined as the average position on the 1D Krylov chain

$$C_{\mathrm{K}}(t) = \sum_n n|\psi_n(t)|^2 = \langle\psi(t)|\mathcal{K}|\psi(t)\rangle, \tag{5}$$

where $\mathcal{K} = \sum_n n|K_n\rangle\langle K_n|$ defines the "complexity operator." This quantity is basis dependent, in a similar way to some quantum coherence monotones [73]. Equation (5) will be our definition of quantum state complexity. To compare it with momentum, we need a precise setup that we introduce next.

Setup. The AdS/CFT correspondence states that the Hilbert space $\mathcal{H}_{\mathrm{CFT}}$ and the dynamics of certain (holographic) CFTs are equivalent to the Hilbert space $\mathcal{H}_{\mathrm{AdS}}$ and dynamics of excitations in AdS. In particular, for semiclassical states, such as the vacuum or thermal states, if one considers excitations generated by primary operators $\mathcal{O}$, their Heisenberg evolution $\mathcal{O}(t) = e^{iHt}\mathcal{O}e^{-itH}$ should be encoded in a relevant Krylov subspace of the full $\mathcal{H}_{\mathrm{CFT}}$. One expects the gravitational dual description of such excitations to be approximately given by propagating bulk particles in an AdS geometry. In fact, it was realized in [74] that 2-pt CFT correlation functions were determined by appropriate bulk geodesics in the large mass approximation. The question we are asking is: how is the spread complexity of the operator in the CFT encoded in the motion of such a bulk particle?

To make this quantitative, we consider the evolution of locally excited states by primary operators in holographic CFTs [75,76]

$$|\psi(t)\rangle = \mathcal{N}e^{-iHt}e^{-\epsilon H}\mathcal{O}(x_0)|\psi_\beta\rangle, \tag{6}$$

where $\mathcal{N}$ is a normalization of the state, $\mathcal{O}$ is a local primary operator of dimension $\Delta = h + \bar{h}$ inserted at spatial position $x = x_0$, $\beta = 1/T$ is the inverse temperature, and $|\psi_\beta\rangle$ can be thought of as a purification of the thermal state (the thermofield-double state) [77].

The ϵ regularization (smearing) in (6) is necessary for $|\psi(t)\rangle \in \mathcal{H}_{\mathrm{CFT}}$ and to have finite energy

$$E_0 = \int dx\langle\psi(t)|T_{00}(x)|\psi(t)\rangle = \frac{\Delta}{\epsilon}. \tag{7}$$

The CFT dynamics of this state describes an entangled pair of excitations propagating to the left and to the right of $x = x_0$ at the speed of light [78]. This wave function spreading will be encoded by the Krylov probabilities $|\psi_n(t)|^2$ solving (3). To study the validity of (1), we will rely on the well-established holographic description of the state (6) in terms of massive point particles in AdS developed in [76,78,79]. Supplemental Material [80] contains more details (see also Refs. [81–86] therein).

Consider first the limit $\beta \to \infty$, so that $|\psi_\beta\rangle \to |0\rangle$ corresponds to the vacuum on the plane, whose semiclassical dual description is given by the Poincaré AdS_3 geometry

$$ds^2 = \frac{-dt^2 + dx^2 + dz^2}{z^2}. \tag{8}$$

The insertion of the local operator $e^{-\epsilon H}\mathcal{O}(x_0)$ at $t = 0$ corresponds to (is "dual" to) a localized point particle in the bulk with mass $m \simeq \Delta$, for $\Delta \gg 1$ and $\epsilon \ll 1$, located at $x = x_0$ and $z = \epsilon$, with vanishing velocity [78,85]. As time evolves, this bulk particle follows a radial timelike geodesic $\{z(t), x = x_0\}$, as shown in Fig. 1.

Geodesics are computed by extremizing the world-line particle action

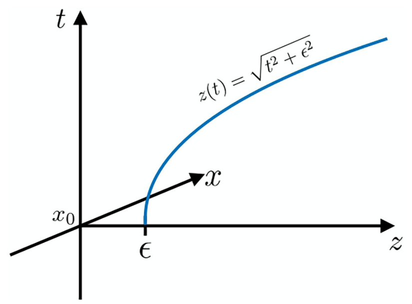

FIG. 1. Holographic dual of a state excited by a local operator (6) corresponds to a massive particle following a timelike geodesic in AdS_3. Here we show the example of an excitation to the CFT vacuum on a line and the corresponding geodesic in (8).

$$S_{\text{particle}} = -m \int d\tau = -m \int d\lambda \sqrt{-g_{\mu\nu}(x)\dot{x}^{\mu}\dot{x}^{\nu}}, \quad (9)$$

describing the particle motion $x^{\mu}(\lambda)$ in a fixed spacetime metric with local components $g_{\mu\nu}(x)$. With the metric (8), working in the gauge $\lambda = t$, (9) becomes

$$S_m = -m \int \frac{\sqrt{1 - \dot{z}(t)^2}}{z(t)} dt. \quad (10)$$

The particle following the on-shell geodesic satisfying our initial condition,

$$z(t) = \sqrt{t^2 + \epsilon^2}, \quad (11)$$

carries the same energy as the CFT excitation (7).

An analogous picture holds for finite β, or $\beta = iL$, by replacing the bulk metric (8) with an AdS black hole or global AdS, i.e., mapping the initial quantum state $|\psi_\beta\rangle$ to its proper semiclassical bulk description. In the black hole background, the point particle falls from the boundary toward the horizon region, which is reached after the time scale $t \sim \beta/2\pi$ [81].

Spread complexity of local operators. To compute the rate of growth of the spread complexity of states (6), we first need to extract the Lanczos coefficients from the return amplitude. In our setups, return amplitudes can be universally determined in terms of ratios of two-point correlators of local operators $\mathcal{O}$. Supplemental Material [80] contains more details (see also Refs. [87–90] therein). At finite temperature, the amplitude is

$$S(t) = \left(\frac{\sinh(\frac{\pi(t+2i\epsilon)}{\beta})}{\sinh(\frac{2\pi i\epsilon}{\beta})} \right)^{-2\Delta}. \quad (12)$$

The corresponding Lanczos coefficients are given by

$$a_n = \frac{2\pi(n+\Delta)}{\beta \tan(\frac{2\pi\epsilon}{\beta})}, \qquad b_n = \frac{\pi\sqrt{n(n+2\Delta-1)}}{\beta \sin(\frac{2\pi\epsilon}{\beta})}. \quad (13)$$

These are examples of the analytical Lanczos coefficients governed by $\mathrm{SL}(2,\mathbb{R})$ symmetry on the Krylov chain [88,91]. The corresponding wave functions are computed in Supplemental Material [80], allowing us to find the spread complexity

$$C_{\mathrm{K}}(t) = \frac{\Delta\beta^2}{2\pi^2\epsilon^2} \sinh^2\left(\frac{\pi t}{\beta}\right), \quad (14)$$

and its rate of growth

$$\dot{C}_{\mathrm{K}}(t) = \frac{E_0}{\epsilon} \frac{\beta}{2\pi} \sinh\left(\frac{2\pi t}{\beta}\right). \quad (15)$$

It is interesting to observe that the characteristic timescale $t \sim \beta/2\pi$ after which the rate grows exponentially matches the time it takes the dual point particle to reach the near-horizon region.

Proceeding in an analogous way, the growth rates of spread complexity for excited states (6) in a CFT of finite size L and on an infinite line are

$$\dot{C}_{\mathrm{K}}(t) = \frac{E_0}{\epsilon} \frac{L}{2\pi} \sin\left(\frac{2\pi t}{L}\right), \qquad \dot{C}_{\mathrm{K}}(t) = \frac{E_0}{\epsilon} t. \quad (16)$$

Together with (15), these are our main CFT results for spread complexity rates. Next, we discuss how to match them with the proper momentum in AdS.

Proper bulk momentum. Given a metric with radial coordinate r [e.g., z in (8)] and trajectory $r(t)$, the radial momentum is the canonical momentum

$$P_r = \frac{\partial \mathcal{L}}{\partial \dot{r}(t)}. \quad (17)$$

Applying this definition to (10) and using (11), one obtains

$$P_z = \frac{mt}{\epsilon\sqrt{t^2 + \epsilon^2}}. \quad (18)$$

Translating mass to CFT data, $m = \Delta$, we get a mismatch with the second formula in (16). At early times the radial momentum grows linearly with t, but it approaches a constant at late times, unlike (16).

Fortunately, there is an elegant way to correct this. The effective 2D geometry probed by the infalling particle is locally AdS_2, whose isometry group $\mathrm{SL}(2,\mathbb{R})$ matches the symmetry controlling the Krylov states $|K_n\rangle$. Small diffeomorphisms preserve the $\mathrm{SL}(2,\mathbb{R})$ symmetry, and so naturally one wonders whether a different choice of radial coordinate could precisely encode the choice of the Krylov basis, which is forced on us by the definition of the spread complexity, and thus capture the spread of the wave function along the Krylov chain. Under the coordinate transformation $z = f(r)$, the radial momentum is given by

$$P_r = \frac{mt}{\epsilon}\frac{f'(r)}{f(r)}. \tag{19}$$

Taking $z = e^{-\rho}$, we find an exact match

$$P_\rho = -\frac{m}{\epsilon}t \Rightarrow \dot{C}_K(t) = -\frac{P_\rho}{\epsilon}. \tag{20}$$

We find an analogous radial coordinate ρ for all the examples (6). Namely, we can write the dual gravity backgrounds to the thermal state as well as to the finite and infinite size vacua as

$$ds^2 = d\rho^2 + \frac{4\pi^2}{\beta^2}(-\sinh^2(\rho)dt^2 + \cosh^2(\rho)dx^2), \tag{21}$$

$$ds^2 = d\rho^2 + \frac{4\pi^2}{L^2}(-\cosh^2(\rho)dt^2 + \sinh^2(\rho)d\phi^2), \tag{22}$$

$$ds^2 = d\rho^2 + e^{2\rho}(-dt^2 + dx^2). \tag{23}$$

In all of them, the radial momentum (17) conjugate to ρ satisfies the second equation in (20). Their common feature is that the radial coordinate ρ computes the *proper* distance to the black hole horizon (21) [analogously to the center of global AdS (21) and to the Poincaré horizon (23), as discussed in Supplemental Material [80] (see also Ref. [92] therein)]. For this reason, we refer to P_ρ as the *proper momentum*.

To check the above claim, consider the timelike geodesic followed by an infalling particle in the black hole background (21)

$$\tanh\rho(t) = \frac{\tanh(\rho_\Lambda)}{\cosh(\frac{2\pi t}{\beta})}. \tag{24}$$

The particle's initial position is related to the ϵ regulator by $\rho_\Lambda = \log(\beta/(\pi\epsilon))$. It follows that the proper radial momentum is

$$P_\rho = \frac{\partial\mathcal{L}}{\partial\dot{\rho}(t)} = -\frac{m}{\epsilon}\frac{\beta}{2\pi}\sinh\left(\frac{2\pi t}{\beta}\right). \tag{25}$$

An analogous computation can be performed for the massive particle in global AdS_3 with metric (22). The particle's trajectory in this case satisfies

$$\tanh(\rho(t)) = \cos\left(\frac{2\pi t}{L}\right)\tanh(\rho_\Lambda), \tag{26}$$

with $\rho_\Lambda = \log(L/(\pi\epsilon))$, leading to the proper momentum

$$P_\rho = -\frac{m}{\epsilon}\frac{L}{2\pi}\sin\left(\frac{2\pi t}{L}\right). \tag{27}$$

In all three cases the momentum is negative, since the particle falls from the boundary at $\rho \sim \infty$ toward $\rho \sim 0$. After mapping parameters to CFT data, we find a precise version of (1) relating the rate of growth of the spread complexity in 2D CFTs and the proper radial momentum of dual massive particles in the bulk

$$\dot{C}_K(t) = -\frac{1}{\epsilon}P_\rho(t). \tag{28}$$

The proportionality constant is the finite energy scale over which we regulate the operator. This is the main result of our work and is the first explicit check of the correspondence between the rate of growth of a well-defined complexity in 2D CFTs and the bulk radial momentum.

Discussion and outlook. We now discuss implications of our results and future directions.

First, the Euler-Lagrange equation for the infalling particle in (1) implies that the second derivative of the spread complexity

$$\ddot{C}_K(t) \propto \frac{d}{dt}\left(\frac{\partial\mathcal{L}}{\partial\dot{r}(t)}\right) = \frac{\partial\mathcal{L}}{\partial r}, \tag{29}$$

equals the force in a nonrelativistic system (where $\mathcal{L} = T - V$ for a conservative force: $F(r) = -\frac{dV(r)}{dr}$). This "Newton's law" relates the acceleration of the bulk particle with the acceleration of the spread complexity. This is consistent with the gravitational arguments in [32] and Ehrenfest's theorem for spread complexity [90].

Second, it is natural to speculate on the relation between the discrete Krylov label n and the radial location ρ. As stressed in the main text, there is a single $SL(2,\mathbb{R})$ symmetry determining the Krylov subspace and the 2D effective Lorentzian geometry probed by the infalling particle. This is remarkable since, due to factorization, 2D CFTs are invariant under two copies of $SL(2,\mathbb{R})$. The relation between these algebras and the Krylov one is in general nontrivial. This suggests

$$|K_n\rangle = \sum_{r,s}\Gamma_{n,r,s}|h,r\rangle \otimes |\bar{h},s\rangle, \tag{30}$$

with some nontrivial coefficients $\Gamma_{n,r,s}$. Indeed, time evolution in $\mathcal{H}_{\rm CFT}$ involves the spread of information in terms of left and right entangled excitations. Additionally, from the return amplitude perspective, one could interpret the excitation as a Gaussian around x_0 whose spread increases with time. That is the picture that is described in the bulk and is also captured by the symmetry of the Krylov subspace.

Third, moving away from our approximation, the infalling particle will backreact on the geometry. This will be captured by Einstein's equations

$$R^{\mu\nu} - \frac{1}{2} R g^{\mu\nu} + \Lambda g^{\mu\nu} = 8\pi G_{\rm N} T^{\mu\nu}, \tag{31}$$

where $T^{\mu\nu}$ is the particle's energy-momentum tensor computed from (9). In our setup, we can check that the proper momentum is $P_\rho = \sqrt{-g} T^{0\rho}$. Hence, we can express our main result in terms of spacetime geometry data by either projecting (31) on the above components or employing the gravitational constraints. This may bridge our work, which provides a sharp quantum mechanical definition of complexity in CFTs, with results relating the momentum of a radial shell of matter with the volume variation [36–38].

Fourth, our calculations relate exact quantum mechanical expectation values with classical conjugate momenta. The AdS/CFT correspondence and the symmetry controlling the dynamics of our examples provide some justification for the validity of the matching we reported. However, there is a broader perspective by which we can interpret our results. Since $C_{\rm K}(t) = \langle \psi(t) | \mathcal{K} | \psi(t) \rangle$ and $\mathcal{K} = L_0 - h\mathbf{1}$ within our setup, it follows that

$$\dot{C}_{\rm K}(t) \propto \langle \psi(t) | [\mathcal{K}, H] | \psi(t) \rangle. \tag{32}$$

Since $\mathcal{K}, H \in \mathrm{SL}(2,\mathbb{R}) \simeq \mathrm{SU}(1,1)$, it follows that the derivative $\dot{C}_{\rm K}(t) = \langle \psi(t) | P | \psi(t) \rangle$ for some operator P in this algebra. This result is exact and could be tested in other symmetry setups, including quantum optics, which makes heavy use of the formalism of $\mathrm{SU}(1,1)$ coherent states [93]. In fact, the same $\mathrm{SL}(2,\mathbb{R})$ technology was used in [94] to analytically compute spread complexity $\langle n \rangle$ in the QCD parton model where it is directly related to parton distribution functions measured at LHC.

To test this identity and to partially link with the holographic logic, consider coherent states $|\alpha\rangle$ in a quantum harmonic oscillator. The complexity operator is given by (see [80])

$$\hat{\mathcal{K}} = \frac{(\hat{p} - \langle p_0 \rangle_\alpha)^2}{2m\omega} + \frac{1}{2} m\omega (\hat{x} - \langle x_0 \rangle_\alpha)^2, \tag{33}$$

and its first and second time derivatives, for coherent states satisfying the same initial condition as our infalling particles, $\langle p_0 \rangle_\alpha = 0$, are

$$[\hat{\mathcal{K}}, \hat{H}] = -i\omega \langle x_0 \rangle_\alpha \hat{p}, \qquad [[\hat{\mathcal{K}}, \hat{H}], \hat{H}] = -m\omega^3 \langle x_0 \rangle_\alpha \hat{x}. \tag{34}$$

These are operator equalities that hold beyond expectation values. However, since the harmonic oscillator potential is quadratic, Ehrenfest's theorem ensures that quantum expectation values satisfy the classical equations of motion. Thus, if we had approximated the exact quantum description by a classical one in the right-hand side of these equations, we would have reached the same conclusion. We are envisioning a similar situation holds in our holographic discussion, modulo subtleties due to gravitational physics.

Finally, the relation between the spread complexity and proper radial momentum provides a guiding principle for holographic complexity and operator growth. The examples presented here are only starting points and we expect our relation to hold, at a minimum, in other quench scenarios and in higher dimensional CFTs. We will explore several of these directions in [95].

Acknowledgments. We are grateful to Vijay Balasubramanian, Giuseppe Di Giulio, Javier Magán, Dimitrios Patramanis, and Onkar Parrikar for feedback and comments. J. S. was supported by the Science and Technology Facilities Council (Grant No. ST/X000494/1). B. S. and R. W. M. are supported by Engineering and Physical Sciences Research Council studentships. P. C. and B. C. are supported by the NCN Sonata Bis 9 2019/34/E/ST2/00123 grant. P. C. is supported by the ERC Consolidator Grant No. 101125449 (acronym: QComplexity). B. C. is supported by the NSF of China through Grant No. 12175238.

Views and opinions expressed are however those of the authors only and do not necessarily reflect those of the European Union or the European Research Council. Neither the European Union nor the granting authority can be held responsible for them.

[1] C. E. Shannon, Bell Syst. Tech. J. **28**, 59 (1949).
[2] A. N. Kolmogorov, Int. J. Comput. Math. **2**, 157 (1968).
[3] J. Rissanen, Ann. Stat. **14**, 1080 (1986).
[4] M. A. Nielsen, Quantum Inf. Comput. **6**, 213 (2006).
[5] B. Ethan and V. Umesh, SIAM J. Comput. **26**, 1411 (2006).
[6] W. H. Zurek, *Complexity, Entropy and the Physics of Information* (CRC Press, Boca Raton, 2018).
[7] S. Aaronson, arXiv:1607.05256.
[8] D. Aharonov and L. Eldar, in *Proceedings—2011 IEEE 52nd Annual Symposium on Foundations of Computer Science, FOCS 2011* (IEEE Computer Society, Northwest Washington, Washington, D.C., 2011), pp. 334–343.
[9] T. J. Osborne, Rep. Prog. Phys. **75**, 022001 (2012).
[10] P. Caputa, N. Kundu, M. Miyaji, T. Takayanagi, and K. Watanabe, J. High Energy Phys. 11 (2017) 097.
[11] R. Jefferson and R. C. Myers, J. High Energy Phys. 10 (2017) 107.

[12] S. Chapman, M. P. Heller, H. Marrochio, and F. Pastawski, Phys. Rev. Lett. **120**, 121602 (2018).
[13] P. Caputa and J. M. Magan, Phys. Rev. Lett. **122**, 231302 (2019).
[14] N. Chagnet, S. Chapman, J. de Boer, and C. Zukowski, Phys. Rev. Lett. **128**, 051601 (2022).
[15] B. Chen, B. Czech, and Z.-z. Wang, Phys. Rev. D **103**, 026015 (2021).
[16] V. Balasubramanian, M. Decross, A. Kar, and O. Parrikar, J. High Energy Phys. 01 (2020) 134.
[17] J. Cotler, N. Hunter-Jones, J. Liu, and B. Yoshida, J. High Energy Phys. 11 (2017) 048.
[18] F. G. S. L. Brandão, W. Chemissany, N. Hunter-Jones, R. Kueng, and J. Preskill, PRX Quantum **2**, 030316 (2021).
[19] J. Haferkamp, P. Faist, N. B. T. Kothakonda, J. Eisert, and N. Y. Halpern, Nat. Phys. **18**, 528 (2022).
[20] A. Munson, N. B. T. Kothakonda, J. Haferkamp, N. Y. Halpern, J. Eisert, and P. Faist, PRX Quantum **6**, 010346 (2025).
[21] A. R. Brown, M. H. Freedman, H. W. Lin, and L. Susskind, Nature (London) **622**, 58 (2023).
[22] A. R. Brown, Nat. Phys. **19**, 401 (2023).
[23] A. Bouland, B. Fefferman, and U. Vazirani, arXiv:1910.14646.
[24] L. Susskind, Fortschr. Phys. **64**, 24 (2016); **64**, 44(A) (2016).
[25] J. M. Maldacena, Adv. Theor. Math. Phys. **2**, 231 (1998).
[26] D. Stanford and L. Susskind, Phys. Rev. D **90**, 126007 (2014).
[27] A. R. Brown, D. A. Roberts, L. Susskind, B. Swingle, and Y. Zhao, Phys. Rev. Lett. **116**, 191301 (2016).
[28] A. Belin, R. C. Myers, S.-M. Ruan, G. Sárosi, and A. J. Speranza, Phys. Rev. Lett. **128**, 081602 (2022).
[29] L. V. Iliesiu, M. Mezei, and G. Sárosi, J. High Energy Phys. 07 (2022) 073.
[30] L. Susskind and Y. Zhao, arXiv:1408.2823.
[31] L. Susskind, arXiv:1802.01198.
[32] L. Susskind, Front. Phys. **8**, 262 (2020).
[33] A. R. Brown, H. Gharibyan, A. Streicher, L. Susskind, L. Thorlacius, and Y. Zhao, Phys. Rev. D **98**, 126016 (2018).
[34] L. Susskind and Y. Zhao, J. High Energy Phys. 03 (2021) 239.
[35] J. M. Magán, J. High Energy Phys. 09 (2018) 043.
[36] J. L. F. Barbon, J. Martin-Garcia, and M. Sasieta, J. High Energy Phys. 04 (2021) 250.
[37] J. L. F. Barbon, J. Martin-Garcia, and M. Sasieta, Phys. Rev. D **102**, 101901 (2020).
[38] J. L. F. Barbón, J. Martín-García, and M. Sasieta, J. High Energy Phys. 07 (2020) 169.
[39] H. W. Lin and L. Susskind, J. High Energy Phys. 01 (2020) 087.
[40] H. W. Lin, J. Maldacena, and Y. Zhao, J. High Energy Phys. 08 (2019) 049.
[41] The idea that size is momentum-dependent is realised in Feynman's parton model [42], the proper length of a string growing with its momentum [43,44], or the BFSS matrix model [45]. A common feature in all these systems is a description of the quantum state in terms of the number of constituents (partons, string bits or D0-branes, respectively). The larger this number, the larger the momentum. Momentum also controls the variation of circuit complexity when evaluated as geodesic length in the space of unitaries [46] and considering a change in the final state [47,48]. We thank the anonymous referee for encouraging us to highlight these connections.
[42] R. P. Feynman, Phys. Rev. Lett. **23**, 1415 (1969).
[43] M. Karliner, I. R. Klebanov, and L. Susskind, Int. J. Mod. Phys. A **03**, 1981 (1988).
[44] L. Susskind, Phys. Rev. D **49**, 6606 (1994).
[45] T. Banks, W. Fischler, S. H. Shenker, and L. Susskind, Phys. Rev. D **55**, 5112 (1997).
[46] M. A. Nielsen, M. R. Dowling, M. Gu, and A. C. Doherty, Science **311**, 1133 (2006).
[47] A. Bernamonti, F. Galli, J. Hernandez, R. C. Myers, S.-M. Ruan, and J. Simón, Phys. Rev. Lett. **123**, 081601 (2019).
[48] A. Bernamonti, F. Galli, J. Hernandez, R. C. Myers, S.-M. Ruan, and J. Simón, J. Phys. A **53**, 29 (2020).
[49] S. Gopalakrishnan, D. A. Huse, V. Khemani, and R. Vasseur, Phys. Rev. B **98**, 220303 (2018).
[50] V. Khemani, D. A. Huse, and A. Nahum, Phys. Rev. B **98**, 144304 (2018).
[51] C. von Keyserlingk, T. Rakovszky, F. Pollmann, and S. Sondhi, Phys. Rev. X **8**, 021013 (2018).
[52] D. E. Parker, X. Cao, A. Avdoshkin, T. Scaffidi, and E. Altman, Phys. Rev. X **9**, 041017 (2019).
[53] S. Sachdev and J. Ye, Phys. Rev. Lett. **70**, 3339 (1993).
[54] A. Kitaev, Talks at KITP, April 7, 2015 and May 27.
[55] X.-L. Qi and A. Streicher, J. High Energy Phys. 08 (2019) 012.
[56] D. A. Roberts, D. Stanford, and A. Streicher, J. High Energy Phys. 06 (2018) 122.
[57] P. Nandy, A. S. Matsoukas-Roubeas, P. Martínez-Azcona, A. Dymarsky, and A. del Campo, Phys. Rep. **1125–1128**, 1 (2025).
[58] J. L. F. Barbón, E. Rabinovici, R. Shir, and R. Sinha, J. High Energy Phys. 10 (2019) 264.
[59] E. Rabinovici, A. Sánchez-Garrido, R. Shir, and J. Sonner, J. High Energy Phys. 06 (2021) 062.
[60] E. Rabinovici, A. Sánchez-Garrido, R. Shir, and J. Sonner, J. High Energy Phys. 07 (2022) 151.
[61] A. Dymarsky and M. Smolkin, Phys. Rev. D **104**, L081702 (2021).
[62] S.-K. Jian, B. Swingle, and Z.-Y. Xian, J. High Energy Phys. 03 (2021) 014.
[63] N. Hörnedal, N. Carabba, A. S. Matsoukas-Roubeas, and A. del Campo, Commun. Phys. **5**, 207 (2022).
[64] R. Basu, A. Ganguly, S. Nath, and O. Parrikar, J. High Energy Phys. 05 (2024) 264.
[65] V. Balasubramanian, J. M. Magan, and Q. Wu, Phys. Rev. D **107**, 126001 (2023).
[66] V. Balasubramanian, J. M. Magan, and Q. Wu, Phys. Rev. E **111**, 014218 (2025).
[67] J. M. Magán and J. Simón, J. High Energy Phys. 05 (2020) 071.
[68] V. Balasubramanian, P. Caputa, J. M. Magan, and Q. Wu, Phys. Rev. D **106**, 046007 (2022).
[69] H. W. Lin, J. High Energy Phys. 11 (2022) 060.
[70] E. Rabinovici, A. Sánchez-Garrido, R. Shir, and J. Sonner, J. High Energy Phys. 08 (2023) 213.

[71] V. S. Viswanath and G. Müller, *The Recursion Method: Application to Many-Body Dynamics* (Springer, Berlin, Heidelberg, Germany, 1994).

[72] C. Lanczos, J. Res. Natl. Bur. Stand. B **45**, 255 (1950).

[73] T. Baumgratz, M. Cramer, and M. B. Plenio, Phys. Rev. Lett. **113**, 140401 (2014).

[74] V. Balasubramanian and S. F. Ross, Phys. Rev. D **61**, 044007 (2000).

[75] M. Nozaki, T. Numasawa, and T. Takayanagi, Phys. Rev. Lett. **112**, 111602 (2014).

[76] P. Caputa, M. Nozaki, and T. Takayanagi, Prog. Theor. Exp. Phys. **2014**, 093B06 (2014).

[77] Results for the vacuum state in a CFT on the infinite line and on a circle of size L are obtained by taking $\beta \to \infty$ and, formally, $\beta \to iL$, respectively. This is why we focus on finite β in the main text. See Supplemental Material for further details.

[78] M. Nozaki, T. Numasawa, and T. Takayanagi, J. High Energy Phys. 05 (2013) 080.

[79] C. T. Asplund, A. Bernamonti, F. Galli, and T. Hartman, J. High Energy Phys. 02 (2015) 171.

[80] See Supplemental Material at http://link.aps.org/supplemental/10.1103/7zs8-9zpg for a review on SL(2,R) methods on spread complexity, the gravity dual description of local CFT operator quenches, the calculation of proper distances in AdS using embedding methods in different coordinate systems and the derivation of spread complexity for coherent states in a harmonic oscillator.

[81] P. Caputa, J. Simón, A. Štikonas, and T. Takayanagi, J. High Energy Phys. 01 (2015) 102.

[82] S. He, T. Numasawa, T. Takayanagi, and K. Watanabe, Phys. Rev. D **90**, 041701 (2014).

[83] P. Calabrese and J. Cardy, J. Stat. Mech. (2016) 064003.

[84] L. Susskind and E. Witten, arXiv:hep-th/9805114.

[85] D. Berenstein and J. Simón, Phys. Rev. D **101**, 046026 (2020).

[86] P. Caputa and G. Di Giulio, J. High Energy Phys. 07 (2025) 164.

[87] P. Caputa, J. M. Magan, and D. Patramanis, Phys. Rev. Res. **4**, 013041 (2022).

[88] P. Caputa, J. M. Magan, D. Patramanis, and E. Tonni, Phys. Rev. D **109**, 086004 (2024).

[89] P. Caputa and S. Datta, J. High Energy Phys. 12 (2021) 188.

[90] J. Erdmenger, S.-K. Jian, and Z.-Y. Xian, J. High Energy Phys. 08 (2023) 176.

[91] A. Dymarsky and A. Gorsky, Phys. Rev. B **102**, 085137 (2020).

[92] M. Banados, C. Teitelboim, and J. Zanelli, Phys. Rev. Lett. **69**, 1849 (1992).

[93] G. S. Agarwal, *Quantum Optics* (Cambridge University Press, Cambridge, England, 2012).

[94] P. Caputa and K. Kutak, Phys. Rev. D **110**, 085011 (2024).

[95] P. Caputa, B. Chen, R. McDonald, J. Simón, and B. Strittmatter (to be published).